DCrownFormer: Morphology-aware Point-to-Mesh Generation Transformer for Dental Crown Prosthesis from 3D Scan Data of Antagonist and Preparation Teeth

Su Yang[1,⋆], Jiyong Han[2,⋆], Sang-Heon Lim[2], Ji-Yong Yoo[1], SuJeong Kim[2], Dahyun Song[2], Sunjung Kim[3], Jun-Min Kim[4,5,⋆⋆], and Won-Jin Yi[1,2,6,⋆⋆]

[1] Applied Bioengineering, Graduate School of Convergence Science and Technology, Seoul National University, Republic of Korea
[2] Interdisciplinary Program in Bioengineering, Graduate School of Engineering, Seoul National University, Republic of Korea
[3] Imaging R&D Center, Osstem Implant Co., LTD, Republic of Korea
[4] Medical Imaging R&D Center, Xcube Co., LTD, Republic of Korea
[5] Electronics and Information Engineering, Hansung University, Republic of Korea
jmkim@hansung.ac.kr
[6] Oral and Maxillofacial Radiology and Dental Research Institute, School of Dentistry, Seoul National University, Republic of Korea
wjyi@snu.ac.kr

Abstract. Dental prosthesis is important in designing artificial replacements to restore the function and appearance of teeth. However, designing a patient-specific dental prosthesis is still labor-intensive and depends on dental professionals with knowledge of oral anatomy and their experience. Also, the initial tooth template for designing dental crowns is not personalized. In this paper, we propose a novel point-to-mesh generation transformer (DCrownFormer) to directly and efficiently generate dental crown meshes from point inputs of 3D scans of antagonist and preparation teeth. Specifically, to learn morphological relationships between a point input and generated points of a dental crown, we introduce a morphology-aware cross-attention module (MCAM) in a transformer decoder and curvature-penalty loss (CPL). Furthermore, we adopt Differentiable Poisson surface reconstruction for mesh reconstruction from generated points and normals of a dental crown by directly optimizing an indicator function using mesh reconstruction loss (MRL). Experimental results demonstrate the superiority of DCrwonFormer compared with other methods, by improving morphological details of occlusal surfaces such as dental grooves and cusps. We further validate the effectiveness of MCAM, MRL, and significant benefits of CPL through ablation studies. The code is available at https://github.com/suyang93/DCrownFormer/.

Keywords: Dental Crown Prosthesis · Point-to-Mesh Generation · Curvature Penalty Loss · Morphology-aware Cross-attention Transformer

⋆ Su Yang and Jiyong Han - These authors contributed equally
⋆⋆ Jun-Min Kim and Won-Jin Yi - These authors are co-corresponding authors

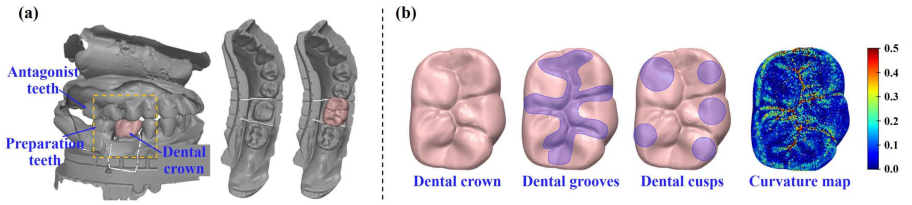

Fig. 1. (a) A 3D scan of antagonist and preparation teeth (grey) along with dental crown (red). The orange dashed line is a region of interest for preparation tooth. (b) Illustration of dental groove and cusp and its normalized absolute curvature map.

1 Introduction

Dental prosthodontics is a branch of dentistry that uses artificial replacements to restore the function and appearance of teeth [1, 2]. When a tooth is damaged or lost due to tooth decay, gum disease, or an accident, a dental prosthesis is designed, fabricated, and implanted to consider the oral anatomy and aesthetics of the tooth [3]. These dental prostheses can be dental crowns, bridges, dentures, or implants, depending on the patient. In general, dental prostheses have similar strength and durability to natural teeth and provide functional and aesthetic help to patients [4].

Dental computer-aided design/computer-aided manufacturing (CAD/CAM) systems led to a significant advancement in digital dentistry, offering a dental solution based on a tooth template for designing dental restorations, including crowns, veneers, bridges, inlays, and onlays. [5–7]. These systems streamline the design and manufacturing process, allowing for accurate and patient-specific dental prostheses. Although the CAD/CAM systems lead to many advantages in digital dentistry, designing a patient-specific dental prosthesis is still labor-intensive and depends on dental professionals with knowledge of oral anatomy and CAD skills [8–10]. Also, the initial tooth template for designing dental restorations is not personalized. It is still time-consuming to fine-tune the position of dental prosthesis taking dental occlusion, ensuring both functionality and aesthetics, and considering harmonious integration with adjacent teeth [9, 10]. Therefore, automatic methods for personalized dental crown design are required to alleviate the workload of a dentist and reduce variability in prosthetic quality.

Recently, artificial intelligence has been used to create dental prostheses in digital dentistry [11, 12, 17]. Farook et al. show that 3D-CNN can be used to generate a partial dental crown. However, 3D-CNN has the limitations of low verification accuracy and precision. Also, a personalizing process is necessary for the use of the standard tooth template [11]. Sukun et al. propose a dual discriminator adversarial learning approach for occlusal surface reconstruction [12]. A depth map was used in this research, however, which makes generating shaded areas difficult. In addition, because antagonistic teeth were not considered, it was not

possible to personalize occlusal surfaces. Hosseinimanesh et al. combined a point completion network [17] with a differentiable surface reconstruction method [19] to generate mesh dental prostheses directly from the point cloud surrounding a prepared tooth. Nevertheless, these methods have some limitations in generating details of a dental mesh including occlusal surfaces such as dental grooves (pits and fissures) and cusps (occlusal or incisal eminences) and the relationship to antagonist teeth, proximal teeth, and a margin line of the preparation tooth.

In this paper, we propose a novel point-to-mesh generation transformer named DCrownFormer to directly and efficiently generate dental crown meshes from point inputs of 3D scans of antagonist and preparation teeth. DCrownFormer has four main components as follows: (1) **Point-to-mesh generation transformer**. To directly generate dental crown meshes from point inputs, we propose a point-to-mesh generation transformer that can capture geometric local-global features of point inputs at the transformer encoder and directly reconstruct fine details of a dental crown mesh at the transformer decoder. (2) **Morphology-aware cross-attention module** (MCAM). We introduce MCAM in a transformer decoder which captures morphological relationships such as dental shapes, scales, and occlusion between a point input and generated points of a dental crown. Point features from a transformer encoder are fed into an MCAM via a skip connection, and a cross-attention layer at each level of an MCAM learns the morphological relationships between encoded point features and decoded point features. (3) **Curvature-penalty loss (CPL)**. We propose CPL to constrain morphological features and details of dental grooves and cusps that affect the functionality, durability, and aesthetics of a dental crown by weighting normalized absolute curvatures at each generated point during the network training. (4) **Mesh reconstruction loss (MRL)**. Motivated by Peng et al. [19], we adopt the Differentiable Poisson surface reconstruction method (DPSR) for mesh reconstruction from generated points and normals of a dental crown and improve the mesh quality of a generated dental crown by directly optimizing an indicator function using MRL without any additional mesh completion layers or models.

2 Method

The overview of our DCrownFormer is shown in Fig. 2. Given an antagonist and preparation tooth scan, we perform uniform point sampling to take a point input $\mathcal{P}_\mathbf{i}$ of size $N \times 3$, where N denotes the number of points. Then a point input $\mathcal{P}_\mathbf{i}$ is fed to the encoder of DCrownFormer to extract a global feature vector $\mathcal{G}$ of size $1 \times 2k$, which captures geometric local-global features of the point input. The decoder of DCrownFormer takes the global feature vector $\mathcal{G}$ to generate points $\mathcal{P}_\mathbf{p}$ and normals $\mathcal{N}_\mathbf{p}$ of a dental crown, where $\mathcal{P}_\mathbf{p}$ and $\mathcal{N}_\mathbf{p}$ has a size $N \times 3$. After generating points $\mathcal{P}_\mathbf{p}$ and normals $\mathcal{N}_\mathbf{p}$ of a dental crown, we use DPSR [19] to directly reconstruct the crown mesh from the points $\mathcal{P}_\mathbf{p}$ and normals $\mathcal{N}_\mathbf{p}$.

Point Feature Encoding. The encoder of DCrownFormer extracts the geometric features in a point input as two global feature vectors $\mathcal{G}_1$ of size $1 \times k$ and $\mathcal{G}_2$ of size $1 \times 2k$, where k denotes an embedding size and set as $k = 256$. It

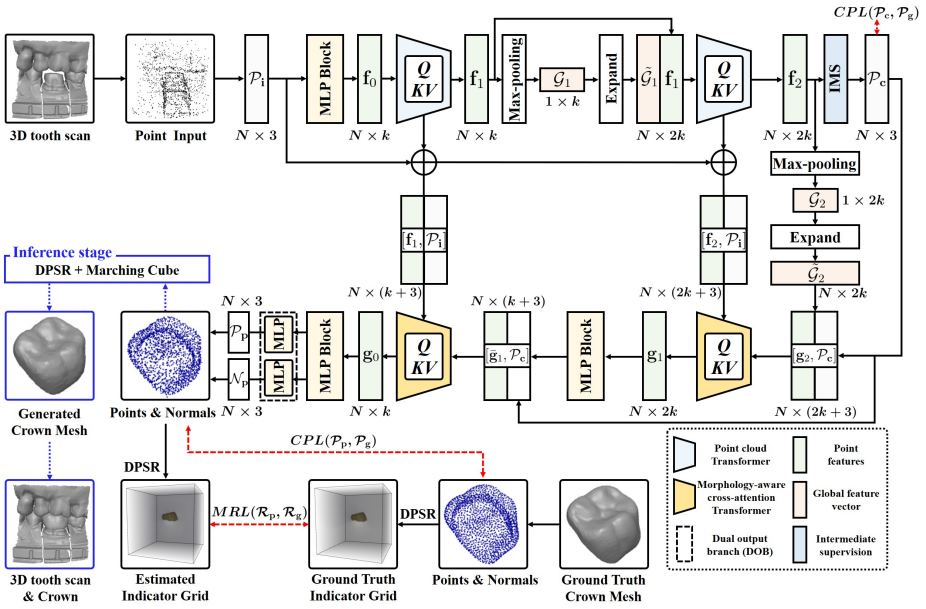

Fig. 2. Illustration of our DCrownFormer architecture. DCrownFormer takes a point input and generates the dental crown mesh by solving the estimated indicator grid.

learns embedding vectors from the antagonist and preparation tooth points to spaces of crown mesh shapes. Specifically, the encoder consists of an MLP block, point cloud transformers (PCT), and point-wise max-pooling (MAP). The MLP block consisting of a shared multi-layer perception layer, Batch normalization (BN), and Rectified Linear Unit (ReLU) activation takes a point input $\mathcal{P}_\mathbf{i}$ where each point has a 3D coordinate (x, y, z) and extracts the point features $\mathbf{f}_0$ size of $N \times k$. Then, PCT consisting of four multi-head self-attention modules [13] is used to capture both short-range and long-range relationships between the point features $\mathbf{f}_0$ and outputs the refined point features $\mathbf{f}_1$. A first global feature vector $\mathcal{G}_1$ is obtained by MAP, where $\mathcal{G}_1^j = \max_{\{i=1,...,N\}}\{\mathbf{f}_1^{ij}\}$ for $j = 1, ..., k$. The global feature vector $\mathcal{G}_1$ expanded to the size of $N \times k$ is concatenated with the point features $\mathbf{f}_1$, and those are fed to the second PCT. The second PCT outputs the fine-grained point features $\mathbf{f}_2$ of size $N \times 2k$ and those are projected by MAP to obtain the second global feature vector $\mathcal{G}_2$ of size $1 \times 2k$. We use four-head self-attention and embedding dimensions of 256 and 512 for each PCT.

Point-to-Mesh Decoding. To directly reconstruct dental crown mesh using DPSR, the decoder of DCrownFormer generates points $\mathcal{P}_\mathbf{p}$ and corresponding normals $\mathcal{N}_\mathbf{p}$ from the expanded global feature vector $\tilde{\mathcal{G}}_2$ of size $N \times 2k$. In our decoder, we adopt MCAM with multi-head cross-attention modules to learn morphological relationships for a balanced dental occlusion between point input and output in a coarse-to-fine manner. The decoder consists of intermediate

supervision (IMS), MCAM, an MLP block, and a dual output branch (DOB). IMS has an MLP layer to generate coarse points $\mathcal{P}_\mathbf{c}$ of size $N \times 3$ from the point features $\mathbf{f}_2$. In our MCAM, Q is obtained from the concatenated decoded point features $\mathbf{g}_n$ and coarse points $\mathcal{P}_\mathbf{c}$. K and V are obtained from the concatenated skip connected point features $\mathbf{f}_n$ and point input $\mathcal{P}_\mathbf{i}$. Our MCAM is defined as:

$$Q = W_i^Q \cdot \text{MLP}([\mathbf{g}_n, \mathcal{P}_\mathbf{c}]), \tag{1}$$

$$K, V = W_i^K \cdot \text{MLP}([\mathbf{f}_n, \mathcal{P}_\mathbf{i}]),\ W_i^V \cdot \text{MLP}([\mathbf{f}_n, \mathcal{P}_\mathbf{i}]), \tag{2}$$

where W_i^Q, W_i^K, and W_i^V are shared learnable linear layers [13], $[\cdot]$ denotes a channel-wise concatenation operation, and MLP is an MLP layer with the embedding dimensions of 256 and 512 at each level of the layer. $\mathbf{f}_n$ and $\mathbf{g}_n$ is skip connected point features from PCT in the encoded and decoded point features at the same level of layer n, respectively. To learn morphological relationships between encoded and decoded point features, we use a cross-attention head $\mathbf{H}_i$ between Q and both K and V by the matrix dot-product operation as follows:

$$\mathbf{H}_i(Q, K, V) = \text{Softmax}(\frac{Q \cdot K^\text{T}}{\sqrt{d_k}}) \cdot V, \tag{3}$$

where d_k is the dimension of the point features. The multi-head cross-attention is defined as $\mathbf{H}(Q, K, V) = W^O \cdot [\mathbf{H}_i, ..., \mathbf{H}_M]_{i=1}^M$, where W^O is a shared learnable linear layer, $[\cdot]$ denotes a concatenation operation, and M is the number of attention head ($M = 4$ in our work). After MCAM, the point features are fed to an MLP block that has the same shape as that of the encoder. Then, we use DOB to generate points $\mathcal{P}_\mathbf{p}$ and normals $\mathcal{N}_\mathbf{p}$ of a dental crown from the final point features $\mathbf{g}_0$, where each branch of DOB has a ReLU and MLP layer.

Curvature-penalty loss. In convex and concave regions with high curvatures, commonly observed in grooves and cusps in a dental crown as shown in Fig. 1(b), Chamfer distance loss (CDL) can lead to a loss of fine details and an over-smoothed out by weighting all points equally [20]. Therefore, we introduce a curvature-penalty CDL called Curvature-penalty loss (CPL) which improves the reconstruction of an occlusal surface and a margin line by assigning normalized absolute curvature weights $|\kappa|$ of size $N \times 1$ to corresponding points as follows:

$$\begin{aligned} CPL(\mathcal{P}_\mathbf{p}, \mathcal{P}_\mathbf{g}) = & \frac{1}{\mid \mathcal{P}_\mathbf{p} \mid} \sum_{x \in \mathcal{P}_\mathbf{p}} e^{\lambda |\kappa(y)|} \min_{y \in \mathcal{P}_\mathbf{g}} \|x - y\|_2^2 + \\ & \frac{1}{\mid \mathcal{P}_\mathbf{g} \mid} \sum_{y \in \mathcal{P}_\mathbf{g}} e^{\lambda |\kappa(y)|} \min_{x \in \mathcal{P}_\mathbf{p}} \|x - y\|_2^2, \end{aligned} \tag{4}$$

where $\mathcal{P}_\mathbf{p}$ and $\mathcal{P}_\mathbf{g}$ are a point output and point ground truth, respectively. λ is a constant value to control the scale of curvature weights. It is noteworthy that in the case of $\lambda = 0$, CPL simplifies to be the same as CDL. $|\kappa(y)|$ is the normalized absolute discrete mean curvature from a point ground truth $\mathcal{P}_\mathbf{g}$ [21, 22]. To normalize the absolute discrete mean curvatures, we empirically set the bound of curvature as $|\kappa(y)| = \min\{|\kappa(y)|, \kappa_{max}\}$, where κ_{max} is set as 5.

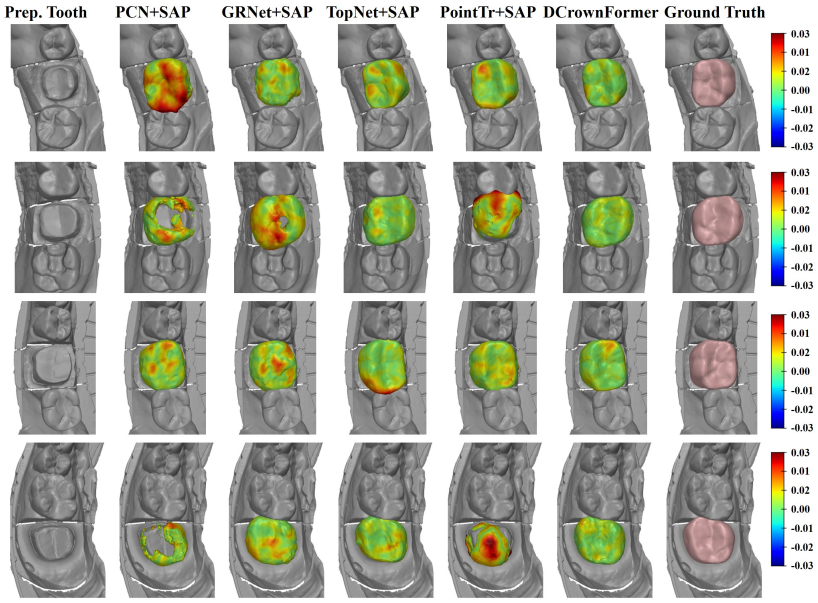

Fig. 3. Visual comparison of different methods for dental crown generation. Color map denotes surface distance error. 3D printing example is given in supplementary Fig. S2.

Mesh reconstruction loss. During training, we minimize MRL consisting of the Mean Square Error (MSE) between the estimated indicator grid $\mathcal{R}_{\mathbf{p}}$ and the indicator grid of ground truth $\mathcal{R}_{\mathbf{g}}$, each obtains using the DPSR [19] from each set of points and normals. The MRL is defined as:

$$MRL(\mathcal{R}_{\mathbf{p}}, \mathcal{R}_{\mathbf{g}}) = \|\mathcal{R}_{\mathbf{p}} - \mathcal{R}_{\mathbf{g}}\|^2, \tag{5}$$

where $\mathcal{R}_{\mathbf{p}}$ and $\mathcal{R}_{\mathbf{g}}$ is calculated by $\mathcal{R}_{\mathbf{p}} = \text{DPSR}(\mathcal{P}_{\mathbf{p}}, \mathcal{N}_{\mathbf{p}})$ and $\mathcal{R}_{\mathbf{g}} = \text{DPSR}(\mathcal{P}_{\mathbf{g}}, \mathcal{N}_{\mathbf{g}})$. Finally, we minimize the total loss L_{total} of CPL and MRL as follows:

$$L_{total} = CPL(\mathcal{P}_{\mathbf{c}}, \mathcal{P}_{\mathbf{g}}) + CPL(\mathcal{P}_{\mathbf{p}}, \mathcal{P}_{\mathbf{g}}) + MRL(\mathcal{R}_{\mathbf{p}}, \mathcal{R}_{\mathbf{g}}). \tag{6}$$

On the inference stage, we estimate the indicator gird $\mathcal{R}_{\mathbf{p}}$ from generated points $\mathcal{P}_{\mathbf{p}}$ and normals $\mathcal{N}_{\mathbf{p}}$ using DPSR and apply Marching cube algorithm [23] to reconstruct dental crown mesh by solving estimated indicator grid $\mathcal{R}_{\mathbf{p}}$.

3 Experiments

3.1 Datasets and Implementation Details

Dataset. We collect a total of 2317 dental plaster cast scans of the antagonist and preparation teeth including mandibular and maxillary molars as shown in Fig. 1(a), using a desktop scanner (D2000, 3Shape, Copenhagen, Denmark). The

Table 1. Performance comparison of DCrownFormer with existing point completion networks combined with SAP. Performance comparison on each tooth is given in the supplementary Table S1.

Methods	CD(↓)	F-score(↑)	NC(↑)	MAE(↓)	R^2(↑)	SDE(↓)
PCN+SAP	18.96±4.38	0.873±0.093	0.761±0.034	4.95±1.80	0.416±0.213	10.37±3.50
GRNet+SAP	17.56±4.05	0.912±0.075	0.629±0.037	5.91±1.81	0.450±0.123	10.83±2.42
TopNet+SAP	18.72±4.84	0.881±0.096	**0.850±0.035**	2.63±0.89	0.526±0.193	8.65±2.76
PointTr+SAP	40.39±25.71	0.605±0.321	0.756±0.070	20.24±62.67	0.351±0.685	17.35±14.40
DCrownFormer	**15.06±3.29**	**0.953±0.062**	0.798±0.047	**1.84±0.53**	**0.694±0.163**	**6.47±2.15**

Table 2. Ablation study results of different components in DCrownFormer.

(a) Ablation study on each component						
Components	CD(↓)	F-score(↑)	NC(↑)	MAE(↓)	R^2(↑)	SDE(↓)
Baseline	15.26±3.18	0.951±0.059	0.775±0.049	2.00±0.64	0.670±0.170	6.65±2.10
Baseline w/ SAM	15.20±3.22	0.952±0.060	**0.809±0.046**	1.72±0.51	0.681±0.169	6.57±2.14
Baseline w/ MCAM (Ours)	**15.06±3.29**	**0.953±0.062**	0.798±0.047	**1.84±0.53**	**0.694±0.163**	**6.47±2.15**
(b) Ablation study on MRL						
Ours w/o *MRL* + SAP	15.38±3.34	0.946±0.065	**0.810±0.034**	4.74±3.52	0.546±0.199	8.03±2.61
Ours w/ *MRL*	**15.06**±3.29	**0.953±0.062**	0.798±0.047	**1.84±0.53**	**0.694±0.163**	**6.47±2.15**

dental crowns corresponding to dental plaster cast scans are designed by a dentist on CAD/CAM dental software (TRIOS, 3Shape, Copenhagen, Denmark). The number of 3D scan data in training, validation, and test datasets was randomly split into 1393, 464, and 460, respectively (Supplementary Fig. S1).

Pre-processing. We extract a region of interest (ROI) mesh cropped to a size of 1.5 cm^3 centered at the preparation tooth which was sufficiently large to include three opposing and two adjacent teeth. After that, a point input was obtained by uniform sampling of 2048 points from an extracted ROI mesh. To generate the ground truth of the indicator grid from a dental crown mesh, we uniformly sample 2048 points and corresponding normals and curvatures from a dental crown mesh and use DPSR with an indicator grid resolution of 128^3 with a Gaussian smoothing parameter of 2 [19]. A point input and the corresponding point ground truth are normalized by shifting the centroid of the point input to the origin and scaling it by the farthest distance from the origin [17].

Traning setup. All models were trained by Adam optimizer for 2000 epochs with an initial learning rate of 10^{-4}. We used a batch size of 16 and an NVIDIA GeForce TITAN X GPU with 24 GB RAM. All models were implemented in Python3 using the PyTorch framework and run on the same computing environments and with the training setup to guarantee a fair comparison.

Evaluation Metrics. We use the Chamfer distance (CD) and F-score with the default threshold of 0.1% to measure the similarity between the predicted and ground truth points [19]. To measure the similarity between predicted and ground truth normals, we measure Normal Consistency (NC) [19]. We also used mean absolute error (MAE) and the coefficient of determination (R^2) to evaluate the similarity between the estimated and ground truth indicator grids. Surface distance error (SDE) is used to evaluate the distance error between the generated and ground truth meshes. CD, MAE, and SDE are displayed by multiplying 10^3.

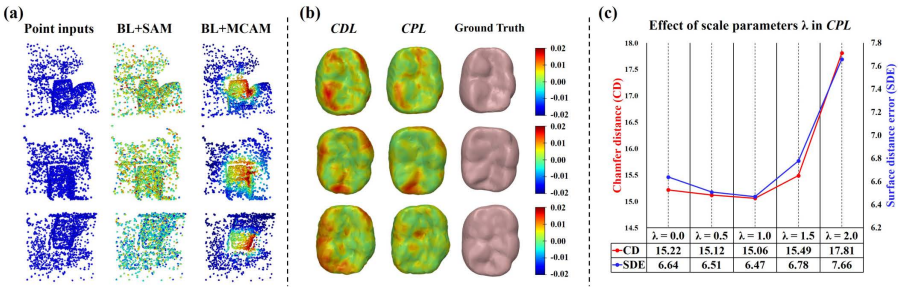

Fig. 4. (a) Point attention maps of Baseline with SAM (BL+SAM) and our Baseline with MCAM (BL+MCAM). (b) Visual comparison of CDL ($\lambda = 0.0$) and CPL ($\lambda = 1.0$). (c) Ablation study results on the effectiveness of scale parameter λ in CPL.

3.2 Experimental Results

Comparison with other methods. We compare DCrownFormer with the four point completion networks [14, 16, 15, 17] integrated with the *Shape As Points* model (SAP) [19] for dental crown reconstruction. Compared with other methods, our DCrownFormer achieves the best performance in all metrics except for NC (Table 1). Specifically, our DCrownFormer surpasses TopNet+SAP with the second-highest performance by obtaining 15.06 ± 3.29, 0.953 ± 0.062, 1.84 ± 0.53, 0.694 ± 0.163, and 6.47 ± 2.15 for CD, F-score, MAE, R^2, and SDE, respectively. As shown in Fig.3, the results of DCrownFormer are relatively close to the ground truth meshes of dental crowns, especially for the morphological structure of the occlusal surface such as the dental grooves and cusps. Compared with the previous state-of-the-art method [18], DCrownFormer shows superior performance in terms of the average CD and F-score.

Component analysis. We perform ablation studies to verify the effectiveness of each component and MRL in DCrownFormer. First, we compare the effectiveness of each component including (1) the Baseline (DCrownFormer without MCAM), (2) the Baseline with a self-attention module (SAM), and (3) the Baseline with MCAM (DCrownFormer). In Table 2(a), our DCrownFormer outperforms the Baseline and the Baseline with SAM. Especially, point attention maps of MCAM are more focused on input points related to the morphology of a dental crown such as the antagonist and proximal teeth, and a margin line than those of SAM as shown in Fig. 4(a). Point attention maps are visualized as point-wise average attention score maps in each last transformer. In Table 2(b), DCrownFormer with MRL outperforms that with SAP by directly optimizing an indicator function without additional mesh completion layers or models.

Effectiveness of scale parameter λ. We evaluate the effectiveness of scale parameter λ of CPL in DCrownFormer as shown in Fig. 4(c). In DCrownFormer, CPL ($\lambda = 1.0$) outperforms CDL ($\lambda = 0.0$) in terms of CD and SDE. When increasing a scale parameter λ from 0.5 to 1.0, the generation performance is higher than that of CDL. While, a further weight on a scale parameter λ (e.g.,

$\lambda > 1.0$), the performance decreases. This result suggests that the scale parameter λ in the proposed CPL needs to be carefully controlled. In Fig. 4(b), we observe that the CPL shows a lower SDE than CDL in DCrownFormer.

4 Conclusion

In this paper, we present a novel point-to-mesh generation transformer named DCrownFormer to directly and efficiently generate dental crown meshes from point inputs of 3D scan data of antagonist and preparation teeth. Our experimental results demonstrate the effectiveness of MCAM and MRL as well as the significant benefits of CPL. Our DCrownFormer also shows superior performance compared to other methods and the previous state-of-the-art method. In future works, We plan to extend our method to directly generate dental meshes of inlay, outlay, and bridges from 3D tooth scan data.

Disclosure of Interests. The authors have no competing interests to declare that are relevant to the content of this article.

Acknowledgments. This work was supported by a grant from the Korea Medical Device Development Fund funded by the Korean government (Ministry of Science and ICT, Ministry of Trade, Industry and Energy, Ministry of Health & Welfare, Ministry of Food and Drug Safety) (Project Number: 1711194231, KMDF-PR-20200901-0011). This work was also supported by a grant from the National Research Foundation of Korea (NRF) funded by the Korean government (MSIT) (No.2023R1A2C200532611).

References

1. Raigrodski, Ariel J., et al.: Survival and complications of zirconia-based fixed dental prostheses: a systematic review. The Journal of prosthetic dentistry, vol. 107(3), pp. 170-177 (2012).
2. Ercoli, Carlo, and Jack G. Caton.: Dental prostheses and tooth-related factors. Journal of periodontology, vol. 89, pp. S223-S236 (2018).
3. Zhao, Jing, Xinzhi Wang. Dental prostheses. In: Advanced ceramics for dentistry, Butterworth-Heinemann, pp. 23-49 (2014).
4. Madfa, Ahmed A., Xiao-Guang Yue.: Dental prostheses mimic the natural enamel behavior under functional loading: A review article. Japanese Dental Science Review, vol. 52.1, pp. 2-13 (2016).
5. Miyazaki, Takashi, et al.: A review of dental CAD/CAM: current status and future perspectives from 20 years of experience. Dental materials journal, vol. 28.1, pp. 44-56 (2009).
6. Davidowitz, Gary, and Philip G. Kotick.: The use of CAD/CAM in dentistry. Dental Clinics, vol. 55.3, pp. 559-570 (2011).
7. Jain, Reeta, et al.: CAD-CAM the future of digital dentistry: a review. Ann Prosthodont Restor Dent, vol. 2, pp. 33-36 (2016).
8. Beuer, Florian, Josef Schweiger, and Daniel Edelhoff.: Digital dentistry: an overview of recent developments for CAD/CAM generated restorations. British dental journal, vol. 204.9, pp. 505-511 (2008).

9. Turkyilmaz, Ilser, Gregory Neil Wilkins, and Giuseppe Varvara.: Tooth preparation, digital design and milling process considerations for CAD/CAM crowns: Understanding the transition from analog to digital workflow. Journal of Dental Sciences, vol. 16.4, 1312 (2021).
10. Chen, Yanning, et al. Morphology and fracture behavior of lithium disilicate dental crowns designed by human and knowledge-based AI. Journal of the Mechanical Behavior of Biomedical Materials, vol. 131, 105256 (2022).
11. Farook, T.H., Ahmed, S., Jamayet, N.B. et al.: Computer-aided design and 3-dimensional artificial/convolutional neural network for digital partial dental crown synthesis and validation. Scientific Reports, vol. 13, 1561 (2023).
12. Tian, Sukun, et al.: A dual discriminator adversarial learning approach for dental occlusal surface reconstruction. Journal of Healthcare Engineering, (2022).
13. Vaswani, Ashish, et al.: Attention is all you need. In: Advances in Neural Information Processing Systems, vol. 30 (2017).
14. Yuan, Wentao, et al. Pcn: Point completion network. In: 2018 international conference on 3D vision (3DV) IEEE, pp. 728-737 (2018).
15. Xie, Haozhe, et al.: Grnet: Gridding residual network for dense point cloud completion. In: European Conference on Computer Vision. Cham: Springer International Publishing, pp. 365-381 (2020).
16. Tchapmi, Lyne P., et al. Topnet: Structural point cloud decoder. In: Proceedings of the IEEE/CVF Conference on Computer Vision and Pattern Recognition, pp. 383-392 (2019).
17. Yu, Xumin, et al.: Pointr: Diverse point cloud completion with geometry-aware transformers. In Proceedings of the IEEE/CVF international conference on computer vision, pp. 12498-12507 (2021).
18. Hosseinimanesh, G., Ghadiri, F., Guibault, F., Cheriet, F., Keren, J.: From Mesh Completion to AI Designed Crown. In: Greenspan, H., et al. Medical Image Computing and Computer Assisted Intervention – MICCAI 2023. MICCAI 2023. Lecture Notes in Computer Science, vol 14228. Springer, Cham (2023). https://doi.org/10.1007/978-3-031-43996-4_53
19. Peng, Songyou, et al.: Shape as points: A differentiable poisson solver. In: Advances in Neural Information Processing Systems, vol. 34, pp. 13032-13044 (2021).
20. Lin, Fangzhou, et al.: Hyperbolic chamfer distance for point cloud completion. In: Proceedings of the IEEE/CVF International Conference on Computer Vision, pp. 14595-14606 (2023).
21. Kim, Sun-Jeong, Kim, Chang-Hun, Levin, David.: Surface simplification using a discrete curvature norm. Computers & Graphics, vol. 26.5, pp. 657-663 (2002).
22. Nealen, Andrew, et al.: Laplacian mesh optimization. In: Proceedings of the 4th international conference on Computer graphics and interactive techniques in Australasia and Southeast Asia, pp. 381-389 (2006).
23. Lorensen, William E., Harvey E. Cline.: Marching cubes: A high resolution 3D surface construction algorithm. In: Seminal graphics: pioneering efforts that shaped the field, pp. 347-353 (1998).